Effects of Pedestrian Pre-Crash Reactions on Crash Outcomes during Multi-body Simulations

Anurag Soni, Thomas Robert, Philippe Beillas

Abstract This study aimed to evaluate the effect of pedestrian pre-crash reactions on injury parameters predicted by simulation. Forty initial conditions arising from simulated accident situations in a volunteer experimental study were used as inputs in car-to-pedestrian multi-body impact simulations. Injury parameters resulting from simulations were then compared with that of a commonly used walking posture. It was found that independent of the choice of crash avoidance strategies, the position of the struck-side leg was having profound effects on the injury predictions and that the existing passive safety procedures were overall a good representation (90th percentile) of the real world pedestrian accident situations.

Keywords car-to-pedestrian impact, multi-body simulations, pedestrian pre-crash reactions

I. INTRODUCTION

Existing passive safety procedures typically do not account for pedestrian pre-crash reactions. Besides subsystem tests, anthropometric test devices or mathematical models used to represent a whole body are typically passive systems configured in the standard walking posture (arms on the sides of the body or tied in the front). The selection of this particular posture which represents only one instance of commonly known pedestrian activities (walking or running) prior to accidents could be compatible with previous epidemiological studies [e.g. 1]. Previous studies [e.g. 2] have simulated variants of walking postures taken from different gait sequences and found pedestrian kinematics and injury outcomes to be significantly affected by the initial conditions. However, while these postures may well represent a walking pedestrian unaware of the imminent accident, they may not represent pedestrians aware of the moving vehicle.

In real life, the perception by the pedestrian of an imminent accident could result in sudden crash avoidance reactions, thus affecting the configuration just prior to impact (pre-crash conditions). In turn, impact and post-impact pedestrian kinematics and injuries could differ from those predicted using procedures based on normal walking postures. It could therefore be useful to assess what consequences pre-crash reactions could have on the passive response and if the normal walking posture could be representative enough to be used to estimate the risk of serious injuries.

Recently, Soni et al. [3] have performed an experimental study to observe volunteer reactions in simulated pedestrian accident situations. Volunteers' postures (in terms of joint angles), speed and orientation were quantified during the events. The current study aims to investigate the possible consequences of these postures on the passive response during an impact with a vehicle and to compare the results with those obtained using the standard walking posture. Numerical simulations of car-to-pedestrian impact were performed using multi-body platform MADYMO^{TM}. Joint angles defining the posture, speed and relative orientation obtained from 40 simulated accident trials were utilized as initial conditions

Anurag Soni, Thomas Robert and Philippe Beillas (Phone: +33 4 72 14 23 71, Fax: +33 4 72 37 68 37 and e-mail: philippe.beillas@ifsttar.fr) are the researchers at the Université de Lyon, F-69622, Lyon, France; IFSTTAR, UMR_T9406, LBMC, Université Lyon 1.

along with a walking posture, and predicted injury parameters were compared across all simulations.

II. METHODS

Pedestrian Pre-Crash Reactions – Volunteer Experiments

In a recent study [3], reactions of volunteers subjected to a simulated accident situation were observed. In the experiments, a street-crossing with two-way traffic flow was simulated using a walking track positioned between two screens onto which generated road traffic was projected using custom software. Volunteers were instructed to cross the street when the traffic permitted it and a simulated accident situation was triggered without their knowledge in order to create a surprise effect. A combination of visual (oncoming truck), audio (brake sound) and physical (air balloon) stimuli was utilized to simulate the accident situation. Volunteers were equipped with 46 Vicon markers that were used to compute postural changes, speed and their orientation with regard to a simulated vehicle front. As a result, forty reactions from twenty three volunteers were obtained which were grouped in three different types of accident avoidance strategies: running, stopped in fright and stepping back. Trajectories obtained from the Vicon motion analysis system were post processed using a custom optimization routine [4] utilizing inverse kinematic solver and joint angles were computed.

Multi-Body Simulations of Car to Pedestrian Impact

Multi-body simulations of car-to-pedestrian impacts, specific to the forty reactions, were performed using the MADYMO 50th percentile pedestrian model and a model of a small sedan [5]. Initial conditions obtained from the volunteer experiments were reproduced in the simulations. Corresponding to each initial condition, angles for the 13 joints of the pedestrian model were altered to define the posture. Additionally, the angle of a global joint called "Human_joint" was altered about the z axis to set the pedestrian orientation relative to the car: a zero value meant a pure lateral impact; a negative value oriented the pedestrian towards the car and a positive angle oriented the pedestrian away from the car. An illustration is provided in the Figure A1 in Appendix A. In addition, an initial speed perpendicular to the car motion was also assigned to the pedestrian model (a positive value was corresponding to forward motion whereas a negative value was corresponding to cases when a pedestrian was stepping back: case 11, 17, 20 and 37 in Table A1 of Appendix A). Details of these parameters for each simulated case are given in Appendix A.

Figure 1 illustrates the simulation setup used in this study. A pedestrian model was configured as standing freely on rigid ground. The coefficient of friction between shoe and ground was set to 0.67. The car model was propelled towards the right side of the pedestrian model with a constant speed of 40 km/h. An acceleration field representing gravity was also applied. In all the simulations, the pedestrian model was placed in front of the car model such that the pedestrian H-point was in the mid plane of the car.

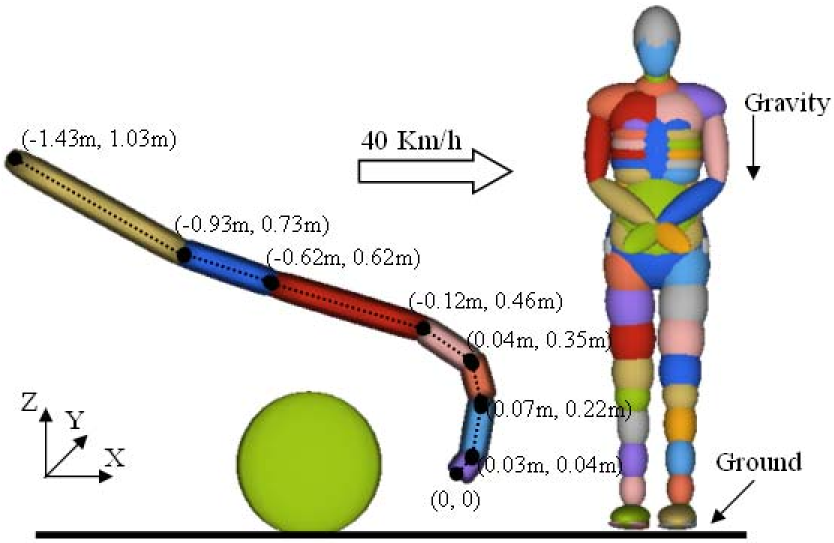

Figure 1: Simulation setup

The contact stiffness curves were characterized by a loading curve (Figure 2) with elastic and plastic parts, and an unloading part was defined using a hysteresis slope. The contact characteristics for the bumper and the bonnet were adopted from stiffness corridors proposed in Martinez et al. [5]. The two parts of the bumper were defined with a single force-deflection curve whereas the bonnet was divided into three different stiffness zones (bonnet leading edge and front were grouped together whereas middle and rear bonnet were defined separately). The car's windscreen is known to have varying stiffness from its center to outer frame. However, in the present study a simplified version of a windscreen model was selected and only a single force-deflection curve was adopted from Mizuno [6]. While it has been shown that local stiffness variations on the windscreen can affect the head impact response, a simplified approach was selected as it allows comparing the effect of initial pedestrian condition at equal stiffness. A coefficient of friction of 0.3 was used to define the friction for all the contacts between the vehicle and the pedestrian [7].

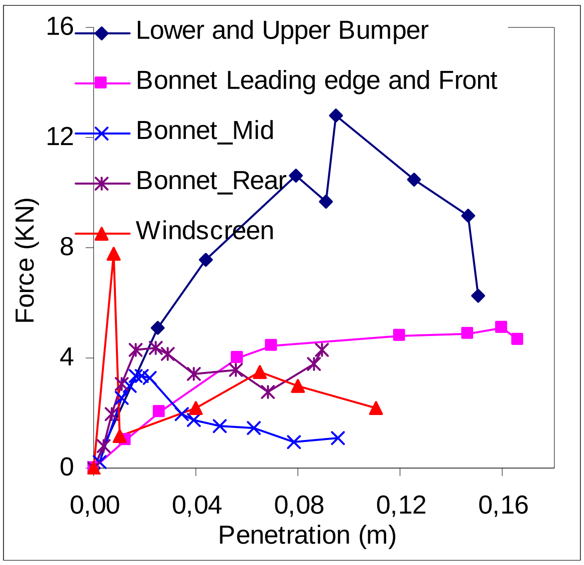

	HYS Slope (N/m)	Elastic Limit(m
Bumper	6.25E+07	0.079
Bonnet Front	6.3E+7	0.056
Bonnet Mid	1.068E+07	0.019
Bonnet Rear	4.3E+07	0.0161
Windscreen	2.2e+07	0.008

Figure 2: Force deflection curves and unloading slopes and elastic limit of different area of the car model used to define their contact characteristics

Simulation was also performed with the pedestrian model configured in a typical walking posture [7] with hands tied in the front. This was considered as the baseline simulation.

Effects of pedestrian pre-crash conditions on the crash outcomes were then investigated by comparing the pedestrian kinematics and injury parameters resulting from these simulations. While head injury criteria over 15 milliseconds (HIC_{15}) was used as an indicator of head injury risk, injury in the struck-side leg was estimated by resultant force and resultant moment in the upper leg at joint 3, knee lateral bending angle and tibia acceleration. Analysis of variance (ANOVA) was also performed to study the influence of the position of the struck side leg (i.e. rear or forward), pedestrian relative orientation (i.e. pure lateral, away or towards the car), pedestrian initial speed, struck side foot support condition and initial impact point on lower extremity (above or below the knee) on the crash outcomes.

III. RESULTS

Forty one simulations were performed successfully. In all simulations, the car bumper initially struck the lower extremity from the lateral side and eventually accelerated the lower leg (see Figure 3). Then the upper and lower legs impacted the front bonnet and the bumper, respectively. Subsequently, both upper and lower leg wrapped around the car front and the feet left the ground. Then, the pelvis hit the bonnet leading edge, leading to the rotation of the upper body. The arm and the thorax then impacted the hood and slid over it. Around 130-180 ms after the initial impact, the head struck the windscreen area. While the head bounced back and left the windscreen, the body continued to rotate. It was observed that both post impact kinematics and injury predicting parameters were dependent on pedestrian pre-impact conditions.

Struck Leg

The position of the struck leg was found to have dominating effects on pedestrian kinematics and resulting head impact conditions. Out of all the cases simulated in this study, the struck leg was in a forward position in 25 cases while it was in a rear position in 16 cases (including the baseline case). In the forward leg impact cases (Figure 3 (a)), initial interaction of the lower extremity with the car front resulted in the upper body rotating away from the car about its longitudinal axis while the pelvis struck and slid against the front bonnet. Eventually, the pedestrian fell on the bonnet on its back with arms wide open and the head struck the windscreen mainly from the posterior aspect. On the contrary, in the rear leg impact cases (Figure 3 (b)), the upper body rotated towards the car about its longitudinal axis which caused the pedestrian to land on the bonnet on its struck side elbow and upper arm, followed by the chest. This led to the head impacting the windscreen on its anterior aspect.

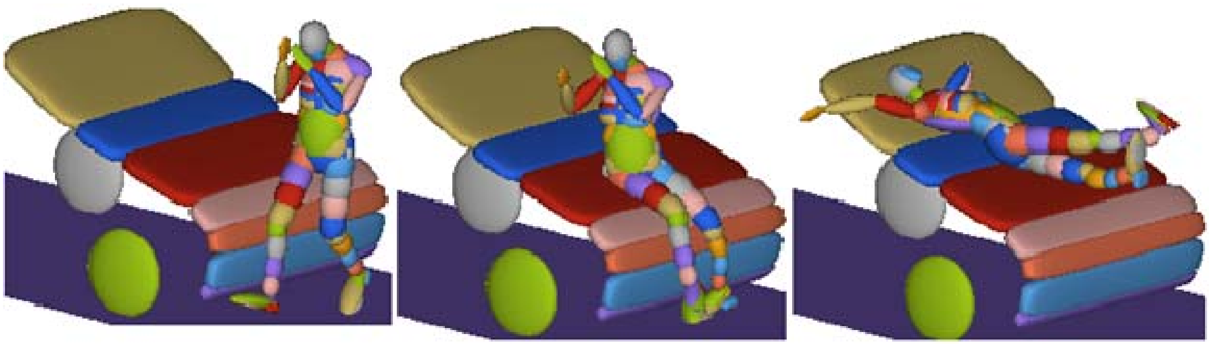

(a)

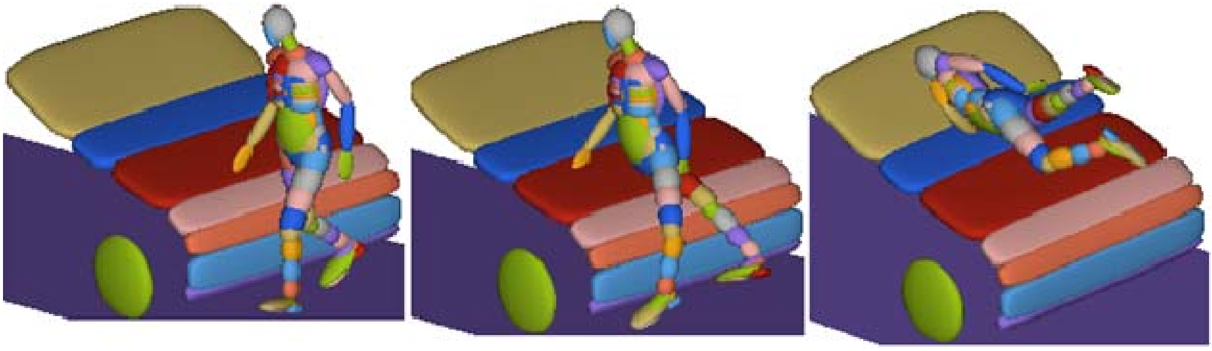

(b)

Figure 3: Comparison of post impact kinematics when struck leg was in (a) forward and (b) rear position

Head Impact Position

The position of the head on the windscreen at impact varied depending upon the pedestrian’s initial conditions (see Figure 4). In the baseline simulation, the head impacted near the windscreen center while in the majority of the remaining cases (28 cases), the head impact location was concentrated in the zone about 20-40 cm left and within 15 cm above the windscreen center. In 10 cases, impact occurred even higher; i.e. in the rearmost 10 cm of the windscreen. Eight of these cases were forward leg impacts and only two were rear leg impacts. These were cases in which pedestrians were experiencing relatively higher speed due to sliding relatively far over the car surface. For example, the pedestrian model in the farthest head landing case (i.e. case 40) was having an initial speed of 3 m/s. It seems that along with the initial speed, a rise in H-point due to pelvic tilt might have contributed in higher follow-up of the pedestrian’s body during the forward leg impact cases. Results of analysis of variance (ANOVA) indicated that the head impact position was mainly affected by pedestrian initial speed (P= 0.013 on windscreen width scale and P = 0.0 on length scale) rather than the position of the struck leg (P = 0.933 on windscreen width scale and P = 0.393 on the length scale).

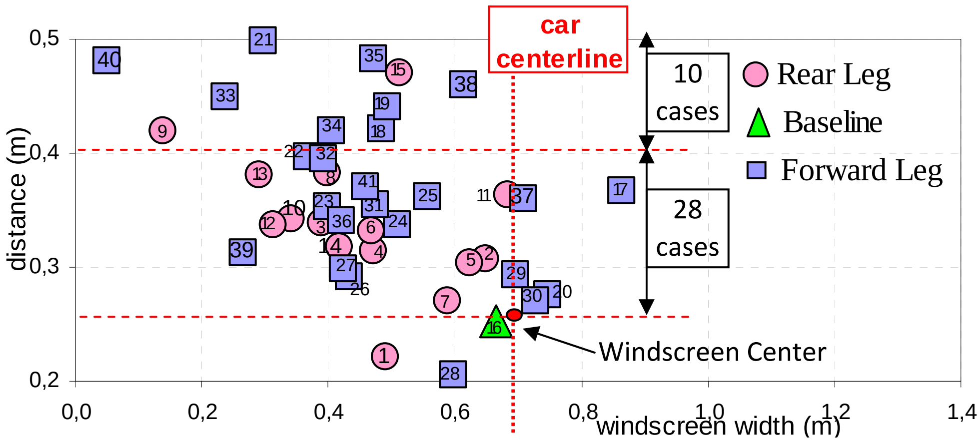

Figure 4: Comparison of head impact positions projected on the top of the windscreen among the 41 simulated cases

Head Injury Criteria

Head injury criteria (HICs) calculated in all the simulated cases are shown in figure 5. Results of ANOVA indicated that the position of the struck side leg, pedestrian initial speed and struck side foot support condition (on the ground or off the ground) seemed to have profound effects (P = 0.004, P =0.0 and P=0.001, respectively) on the resulting HIC values, but pedestrian orientation and initial impact position (above or below the knee) did not seem to have significant effects (P=0.9 and 0.286, respectively). While HIC was found to be highly variable (ranging from 181 to 1327), rear leg impact cases led to higher HIC values than forward leg impact cases. The average HIC estimated in the rear leg impact cases was about 1.7 times higher (920 vs 541) than forward leg impact cases. As compared to the baseline simulation (HIC =1114, case 16 in Figure 5), the HIC value was higher (i.e. 1327, 1123, 1217, 1320 and 1283) in only 5 cases (i.e. 1, 2, 7, 28, and 29, respectively). This implies that as far as estimation of head injuries is concerned, among the simulated cases standard walking posture may be close to a worst case scenario (90th percentile).

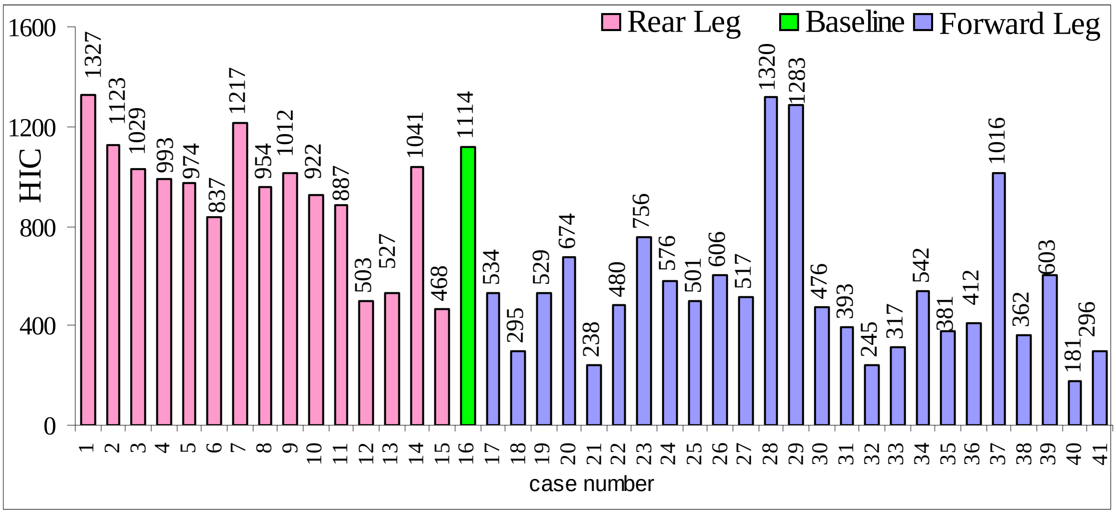

Figure 5: Comparison of HIC among the 41 simulated cases

Head resultant linear impact velocity, angular velocity and angular acceleration (averaged over the time for which HIC was calculated) were plotted against HIC in Figure 6 (a), (b) and (c) respectively. While HIC increased with the increase in head linear impact velocity and average angular acceleration with some exceptions, no such relationship was seen between HIC and head angular velocity.

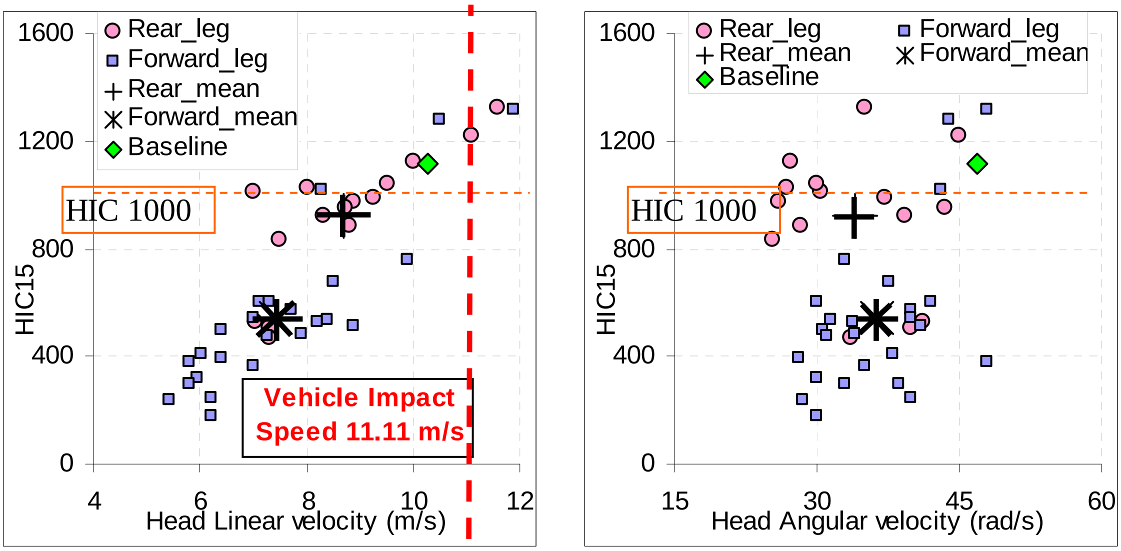

(a) (b)

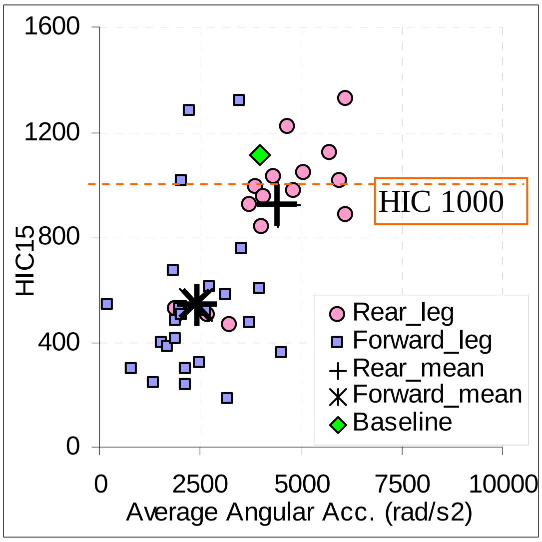

(c)

Figure 6: Comparison of HIC plotted against (a) head linear impact velocity, (b) angular velocity and (c) average angular acceleration

Results of ANOVA indicated that head linear velocity and angular acceleration were significantly affected by both the position of the struck side leg (P= 0.039 and P = 0.0, respectively) and pedestrian initial speed (P = 0.029 and P = 0.0, respectively). Linear velocity of the head varied from 5.44 m/s to 11.9 m/s with two cases attaining head velocity (11.47 m/s in case 1 and 11.9 m/s in case 28) higher than the vehicle speed of 11.11 m/s. Average angular acceleration of the head also varied significantly from 211 rad/s2 to 6120 rad/s2. In general, values of all three kinematic parameters were found lower in the forward leg impact cases as compared to the rear leg impact cases. This could possibly explain the reason for lower HIC values in the forward leg impact cases than the rear leg impact cases. The average values of head linear velocity and angular acceleration in the forward leg impact were lower by 1.25 m/s (7.43 m/s vs 8.62 m/s), and 2048 rad/s2 (2372 rad/s2 vs 4420 rad/s2) as compared to the rear leg impact cases, respectively.

Struck Side Leg

Injuries to the struck side leg were evaluated using resultant peak force (Figure 7 (a)) and resultant peak moment in the upper leg (Figure 7 (b), knee lateral bending angle (Figure 7 (c) and peak tibia acceleration (Figure 7 (d)). All the lower extremity injury predicting parameters seemed to vary corresponding to the simulated initial conditions. Results of ANOVA indicated that support condition of the struck side foot has no significant effects on any of the lower extremity injury predicting parameters (i.e. P = 0.27, 0.28, 0.85 and 0.19 for upper leg force, upper leg moment, knee bending angle and tibia acceleration, respectively) included in this study. Moreover, initial impact position on the lower extremity was found to have significant effects only on the struck side tibia acceleration (P=0.03).

While peak force in the upper leg varied from 2124 N in case 29 to 9983 N in case 13, rear leg impact cases led to lower force values than the forward leg cases. The average value of the peak force in the rear leg cases was 408 N lower than the forward leg cases. In 8 cases, the peak force was above the baseline case (5098 N).

The peak moment in the upper leg varied from 81 N.m (in case 13) to 301 N.m; however, the average values of the peak moment for forward and rear leg impact cases differed by less than 20 N.m (218 N.m vs 200 N.m). The knee lateral bending angle varied from 1.1 deg to 13.3 deg; however, the average values of the peak bending angle for forward and rear leg impact cases differed by less than 0.5 deg (5.53 deg vs 5.11 deg). Moreover, the bending angle was higher than the baseline case (10.1 deg) only in 2 cases (both of which were forward leg cases).

For the tibia, the baseline case accounted for the lowest tibia acceleration (87g) whereas the maximum was higher by more than a factor of two (192g in case 20). On average, forward leg cases sustained higher tibia accelerations than the rear leg cases (129g vs 116g).

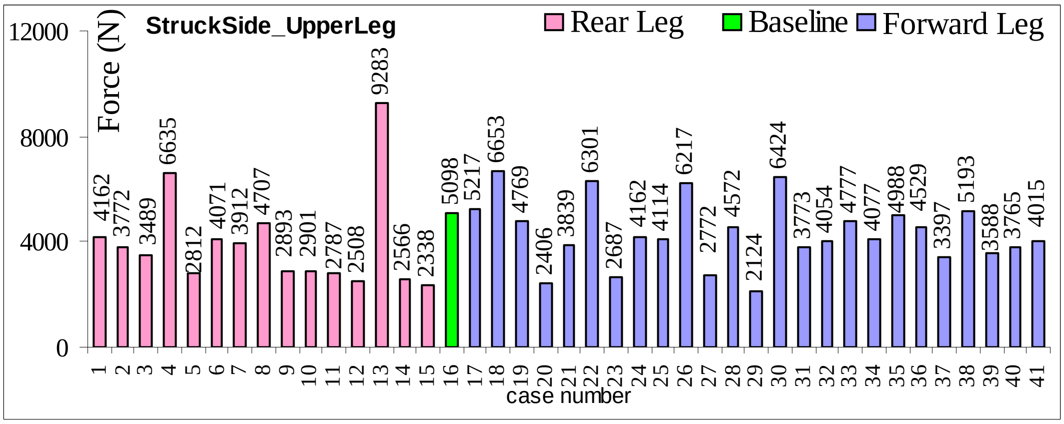

(a)

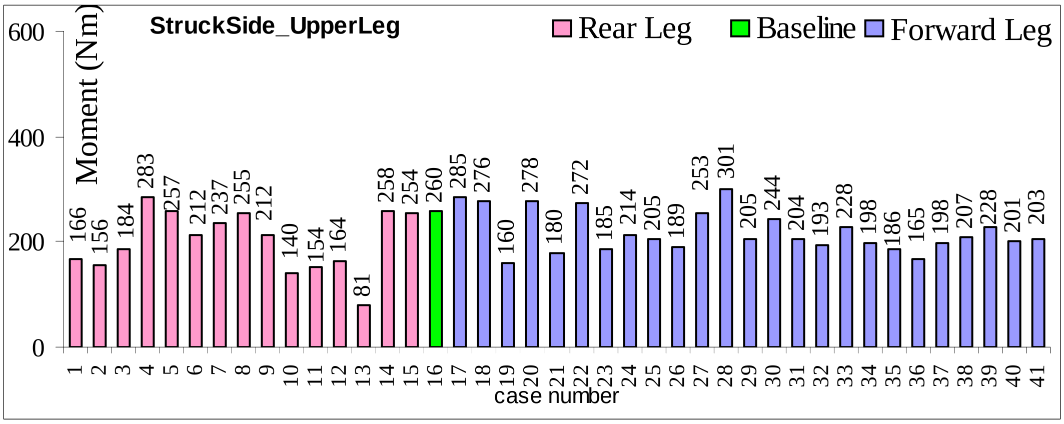

(b)

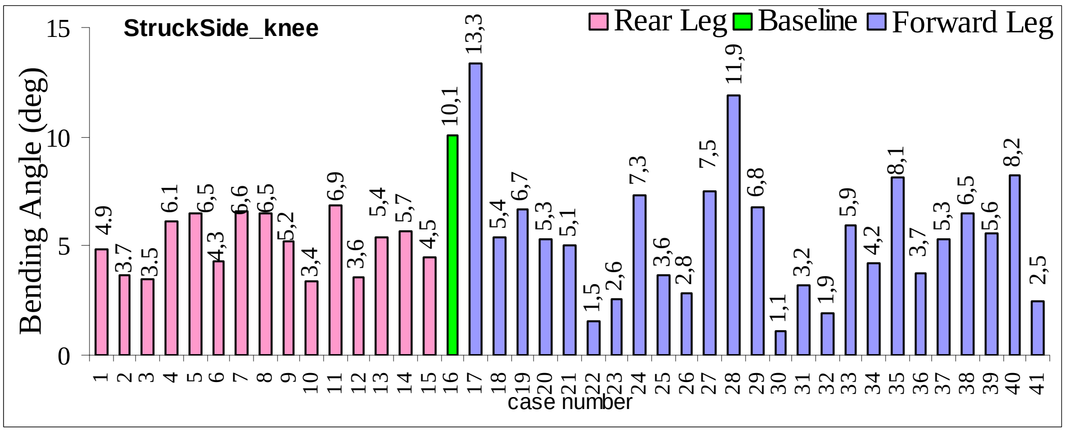

(c)

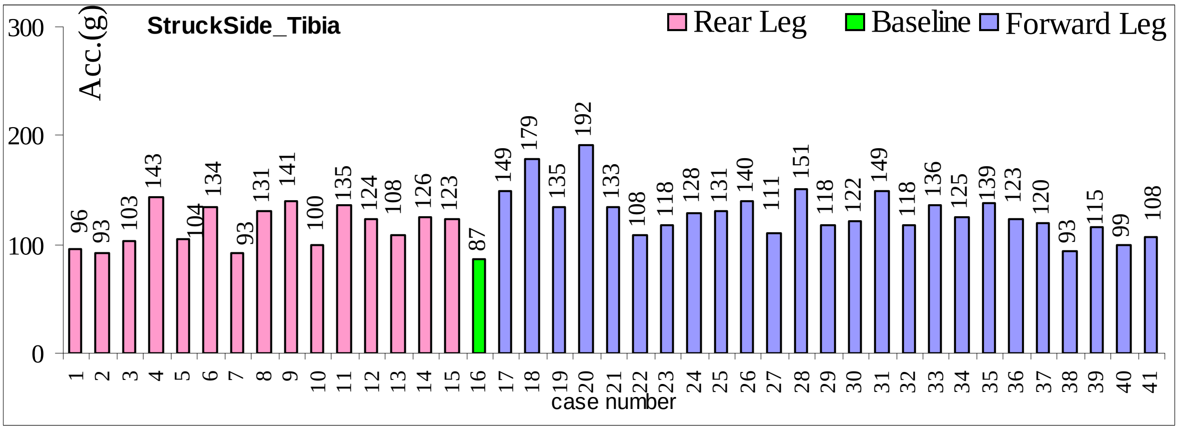

(d)

Figure 7: Comparison of injury parameters in the struck side lower extremity (a) upper leg peak fore, (b) upper leg peak moment (c) knee lateral bending angle and (d) tibia acceleration

IV. DISCUSSION

Forty pedestrian initial conditions corresponding to three different crash avoidance strategies (running, stepping back or freezing in fright) from a volunteer experimental study [3] were utilized in the present work. It seems that crash avoidance strategies could affect pedestrian head impact conditions on the windscreen. For example, higher speed achieved by a pedestrian who started running after the detection of the oncoming vehicle may affect the pedestrian sliding over the bonnet during the impact and eventually the head may impact farther over the windscreen as compared to the cases where the pedestrian either froze in apparent fright or stepped back. In addition, it seems that, irrespective of the crash avoidance strategy, the position of the impacted leg also has profound effects on the crash outcome, particularly for the head. In the rear leg impact, the pedestrian rotated inwards leading to frontal head impact, whereas impact on the forward leg rotated the pedestrian outwards and eventually resulted in rear head impact. HIC, head linear impact velocity and angular acceleration were also substantially higher in the rear leg impact cases as compared to the forward leg impact cases. However, orientation of the head at impact should be considered prior to determining injury risk as types and severity of brain injuries could differ depending upon whether the impact is to the anterior or the posterior aspect of the head [8-11].

Due to high variability posed by the forty initial conditions, a pattern could only be identified for lower extremity position. Moreover, it was not possible to individually evaluate the effects of different parameters affecting the head impact conditions. The differences in head impact conditions between forward and rear leg impact cases could therefore possibly be attributed to the interactions among different parameters such as initial posture (likely to affect the effective moment of inertia), position of struck side leg relative to the car front (likely to affect the initial impact), gaps between the legs, foot support conditions, pedestrian orientation and speed. Position of arms was also seen to have effects particularly in the rear leg impact cases when the pedestrian fell on the bonnet with its arms under the chest but not for the forward impact cases in which the pedestrian fell on the bonnet on its back with arms wide open. In the future, a more detailed principal component analysis could be performed using pedestrian initial conditions utilized here and effects of individual parameters then could further be evaluated.

For the struck side leg, case 13 sustained the highest upper leg force (9283 N) but the least upper leg moment (81 N-m). It was found that after the initial impact the struck side leg was tangled (see Figure 8) between the non struck side leg and the car structure while the upper body was leaning towards the bonnet. This seemed to cause a very high axial extension force (7998 N) as compared to other components (i.e. 4633 N of lateral shear in the direction of car motion and 858 N of shear force in the direction perpendicular to car motion).

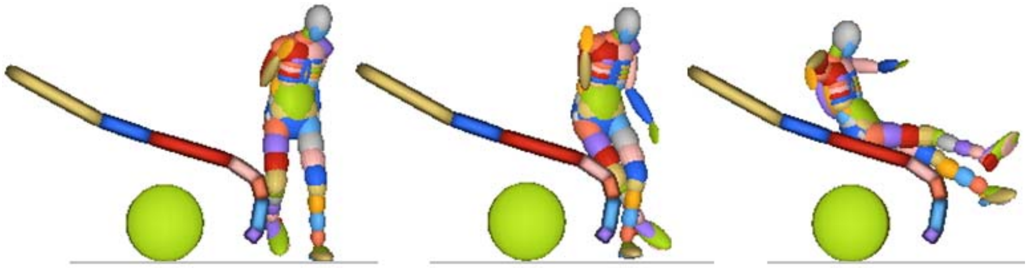

Figure 8: Different stages of pedestrian impact for case 13

Knee lateral bending angle was found to be above 10 degrees for cases 16, 17 and 28 (see Table 1). For all these cases, higher knee bending angle could be related to direct loading on the knee joint (ratio of heights of the first impact point to the knee joint were close to 1). Position of first impact point on the lower extremity (above or below knee impact) was found to significantly affect the tibia acceleration. On average, struck side tibia acceleration was found to be higher when the point of first impact was above (131g +/- 18) the knee joint than below the knee joint (116g +/- 25).

Table 1: Comparison of knee lateral bending angle among the cases 16, 17 and 28

Case ID	Knee Lateral Angle (in degree)	Foot Supported on ground	Height of Knee joint from ground at Time zero (in m)	Height of First Impact point from ground (in m)	Ratio (column 5 / column 4)
16	10.1	Yes	0.45	0.44	0.98
17	13.3	No	0.5	0.51	1.03
28	11.9	Yes	0.48	0.43	0.9

Comparing a baseline case of typical walking posture with the 40 different initial conditions (see Table 2), except the tibia acceleration, the walking posture typically led to high values of injury parameters, typically ranking between 84th percentile and 94th percentile. This indicates that while pedestrian crash avoidance strategies could be important for devising and evaluating active safety systems, the end results of these strategies in terms of pedestrian pre-crash conditions do not seem to affect the overall outcome compared with the standard posture. The avoidance strategies (especially for the running strategy) typically led to impact higher up on the windscreen (increased wrap around distance) which may be important in cases where hard points are present.

Table 2: Comparison of values of injury parameters resulting from baseline simulations and from other simulated cases

	HIC	Head Linear Velocity (m/s)	Head Angular Acc. (rad/s2)	Thigh Force (N)	Thigh Moment (N.m)	Knee Angle (deg)	Tibia Acc. (g)
Baseline	1114	10.27	3980	5098	259	10	86
Percentile of baseline in all simulations	90th	90th	90th	84th	88th	94th	0th
Rear Leg mean +/- (SD)	921 (251)	8.7 (1.41)	4421 (1257)	3922 (1851)	200 (57)	5.11 (1.25)	116 (18)
Forward Leg mean +/- (SD)	541 (291)	7.4 (1.62)	2372 (995)	4336 (1124)	218 (39)	5.53 (3.1)	129 (22)

Also important to mention here is that it is unknown how well the forty initial conditions simulated in the present study represent the field in general, particularly because the experimental approach forced most of the volunteers to react during the experiment. Thus, resulting volunteers' positions may not well represent the positions of unaware pedestrians walking normally (which were already covered by previous studies (e.g. [2]). However, these positions may better represent those situations where the pedestrian was aware of the imminent accident. When considering only that subset (and only based on the experimental results), it appeared that the walking posture was close to the worst case scenario within the subset and thus this posture could be appropriate to estimate an injury risk.

There are several limitations in this study which need to be addressed before drawing definitive conclusions. Results from the present study are specific to the impact configuration representing a small sedan impacting a centrally located pedestrian at 40 km/h. Previous studies [12-17] have shown that outcomes of car-to-pedestrian impact are sensitive to parameters such as car front profile, impact speed and pedestrian position in front of the car. A sensitivity study should therefore be performed to verify if the current results are still valid for other impact configurations.

Although the windscreen of a car is stiffer towards the edges, a single stiffness curve was used to define the entire windscreen. A detailed version of the windscreen model (location dependent stiffness and fracture modeling) could be desirable. However, it would have added extra variables and, consequently, it would have become more difficult to judge/compare whether the resulting head impact variations (and HIC) are due to the changes in initial conditions for the pedestrian or to windscreen modeling parameters (e.g. stiffness dependence to small variations of impact location). It may then have been required to simulate different vehicles/windscreen combinations to avoid introducing a bias due to specific vehicle parameters. Since the main objective was to study the effect of the initial position in general (for equal stiffness parameters), it was felt that a detailed modeling approach was not needed and thus a uniform stiffness was selected.

Knowing that the force, and thus the acceleration, experienced by the head depends upon the force-deformation characteristics, a uniform stiffness approach for modeling the windscreen might have underestimated the HIC and head angular accelerations especially for those cases in which the head impacted near the rearmost edge of the windscreen. Reference [18] also suggested that by doubling the linear stiffness for the windscreen contact, the peak angular and linear accelerations increase by 1.414 times. However, for a nonlinear contact characteristic, as used in the present study, both angular and linear head accelerations could be more sensitive to the change in stiffness. Therefore, one needs to be cautious before interpreting the results, especially the HIC values, for further analysis.

Injury predictive capabilities (such as bone fracture) of MADYMO^{TM} models could not be utilized, primarily to avoid including extra parameters which could affect the crash outcomes. For example, a bone fracture in the lower extremity is known to alter the post impact kinematics, hence affecting the head impact conditions which would make crash outcome evaluation difficult.

V. CONCLUSIONS

Pre-crash data obtained through volunteer experiments were utilized to study the effects of possible pre-crash reactions in pedestrian impacts. Postural and velocity results were used to drive simulations. Based on the simulation results, it can be concluded that initial conditions resulting from the pedestrian crash avoidance reactions have limited effects on the injury parameters compared to parameters as load bearing leg. Among all the initial conditions simulated in the present study, the standard walking posture commonly used for a vehicle passive safety evaluation seems close to a worst case situation.

VI. ACKNOWLEDGEMENT

The research leading to these results has received funding from the European Union Seventh Framework Programme FP7/2007-2013 –International Incoming Fellowship– under grant agreement No [252605]-[PedPcReact].

VII. REFERENCES

[1] Chidester C, Isenberg R, Final Report—the Pedestrian Crash Data Study, *Proceedings of 17th Experimental Safety Vehicle Conference*, paper no. 248, 2001.

[2] Untaroiu CD, Meissner MU, Crandall JR, Takahashi Y, Okamoto M, Ito O, Crash reconstruction of pedestrian accidents using optimization techniques, International *Journal of Impact Engineering*, 36(2):210-19, 2009.

[3] Soni A, Thomas R, Rongiéras F, Beillas P, Observations on pedestrian pre-crash reactions during simulated accidents, paper submitted to *STAPP 2013*.

[4] Wang X, Chevalot N, Monnier G, Ausejo S, Suescun A, Celigüa J, Validation of a model-based motion reconstruction method developed in the REALMAN project, *SAE* Technical Paper 2005-01-2743, 2005, doi:10.4271/2005-01-2743.

[5] Martinez L, Guerra LJ, Ferichola G, Garcia A, Yang J, Yao JF, Stiffness Corridors for the Current European Fleet, APROSYS document APSP31009R, Deliverable D3.1.2.B, 2006.

[6] Mizuno K, Kajzer J, Head injuries in vehicle-pedestrian impact, *Proceedings of Society of Automotive Engineers (SAE) World Congress,* SAE Paper No. 2000-01-0157, 2000.

[7] Mizuno Y, Summary of IHRA Pedestrian safety WG activities (2003) – proposed test methods to evaluate pedestrian protection afforded by passenger cars, *Proceedings of the 18th ESV Conference*, 2003.

[8] Nahum AM, Smith R, Ward C, Intracranial pressure dynamics during head impact, *Proceedings of 21st Stapp Car Crash Conference*, SAE Paper No. 770922, Society of Automotive Engineers, 1977, Warrendale, PA, pages 337–366.

[9] Gennarelli TA, Thibault LE et al., Directional dependence of axonal brain injury due to centroidal and non-centroidal acceleration, *Proceedings of 31st Stapp Car Crash Conference*, SAE Paper No. 872197, Society of Automotive Engineers, Warrendale, PA, pages 49–53, 1987.

[10] Zhang L, Yang KH, King AI, Comparison of brain responses between frontal and lateral impacts by finite element modeling, *J Neurotrauma*, 18(1):21–30, 2001.

[11]Kleiven S, Influence of impact direction to the human head in prediction of subdural hematoma, *J Neurotrauma*, 20(4):365–379, 2003.

[12]Liu XJ, Yang JK, Lövsund P, A study of influences of vehicle speed and front structure on pedestrian impact responses using mathematical models, *Traffic Injury Prevention*, 3(1):31-42, 2002

[13]Longhitano D, Henary B, Bhalla K, Ivarsson J, Crandall J, Influence of vehicle body type on pedestrian injury distribution, *Proceedings of Society of Automotive Engineers (SAE) World Congress*, 2005, SAE, Warrendale, PA, Paper 2005-01-1876.

[14]Kerrigan J, Rudd R, Subit D, Untaroiu C, Crandall J, Pedestrian lower extremity response and injury: a small sedan vs. a large sport utility vehicle, *Proceedings of the SAE World Congress & Exhibition*, 2008; Detroit, MI, Warrendale, Society of Automotive Engineers, SAE 2008-01-1245.

[15]Simms C, Wood D, Pedestrian and Cyclist Impact - a Biomechanical Perspective, *Springer,* 2009

[16]Han Y, Yang J, Mizuno K, Matsui Y, Effects of vehicle impact velocity, vehicle front-end shapes on pedestrian injury risk, *Traffic Injury Prevention*, 13(5):507-18, 2012.

[17]Roséna E, Stigson H, Sandera U, Literature review of pedestrian fatality risk as a function of car impact speed, *Accident Analysis & Prevention*, 43(1): 25–33, 2011.

[18]Lyons M, Simms CK, Predicting the influence of windscreen design on pedestrian head injuries, *Proceedings of IRCOBI Conference,* 2012, Dublin, Ireland, pp. 703-716.

I. APPENDIX – A

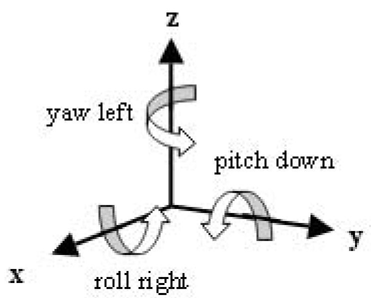

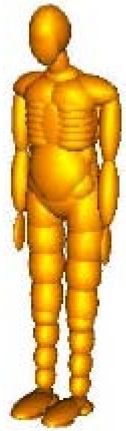

Joint description	Identifier	Degree of freedom		
		D1 / R1	D2 / R2	D3 / R3
Complete human	Human_jnt	X / Roll right	Y / Pitch down	Z / Yaw left
Lower lumbar joint	LumbarLow-LumbarUp_jnt	Yaw right	Pitch down	Roll right
Upper lumbar joint	LumbarUp-TorsoUp_jnt	Roll right	Pitch down	Yaw left
T1	TorsoUp-NeckLow_jnt	Pitch down		
Neck joint	NeckLow-NeckUp_jnt	Roll right	Pitch down	Yaw left
Head OC	NeckUp-Head_jnt	Roll right	Pitch down	Yaw left
Hip	Hip*S*_jnt	Roll right	Pitch down	Yaw left
Knee	Knee*S*_jnt[1)]	Pitch down	Roll left	Yaw left
Ankle	Ankle*S*_jnt	Yaw left	Roll right	Pitch down
Shoulder	Shoulder*S*_jnt	Pitch down	Roll right	
Elbow	Elbow*S*_jnt	Yaw left	Pitch down	
Wrist	Wrist*S*_jnt	Yaw left	Roll right	

[1)] *S* = L or R, stands for left and right side, respectively.

Figure A1: Definition of joint translation and rotation of the pedestrian model. The pedestrian shown is in its reference position.

Table A1: Initial speed (in m/s) and joint angles (in degrees) applied to the pedestrian model for 41 cases simulated in this study. The definition of the joint rotations here is as per MADYMO pedestrian model user manual.

Case	Impact	Initial Speed	Foot Support on Ground	Knee Height from ground at T=0	Height of First Impact Point	Human_Jnt	NeckUp-Head_Jnt		NeckLow_NeckUp_Jnt			TorsoUp_Necklow_Jnt	LumbarUp_TorsoUp_Jnt			_LumbarLow_LumbarUp_Jnt			StruckSide_Shoulder_Jnt		NonStruckSide_Shoulder_Jnt		StruckSide_Elbow_Jnt		NonStruckSide_Elbow_Jnt		StruckSide_Hip_Jnt			NonStruckSide_Hip_Jnt			StruckSide_Knee_Jnt		NonStruckS_Knee_Jı	
Number	Cases	(m/s)	yes	0,45	0,51	R3	R2	R3	R1	R2	R3	R1	R1	R2	R3	R1	R2	R3	R1	R2	R1	R2	R1	R2	R1	R2	R1	R2	R3	R1	R2	R3	R2	R3	R1	R2
1		1,59	yes	0,43	0,49	0	0	0	28	5	-31	6	0	0	0	0	-15	0	29	-23	10	27	27	-26	-43	-20	4	9	-1	6	-35	10	8	-16	0	6
2		0,42	yes	0,44	0,44	-17	0	0	22	3	-24	-7	-1	6	-4	29	-15	-2	0	-17	0	17	46	-120	-46	-120	2	3	8	-7	-20	12	30	-40	0	5
3		1,54	no	0,46	0,39	0	0	0	5	4	-20	5	0	0	1	0	-8	0	15	-22	32	17	40	-28	-33	-24	-4	3	1	1	-30	12	24	-27	0	28
4		1,35	yes	0,44	0,50	9	0	0	17	-1	-10	10	1	0	0	0	-12	1	-4	-14	23	24	-157	36	-21	-52	-3	8	2	-1	-3	27	56	-20	0	29
5		0,00	yes	0,47	0,46	0	0	0	18	-11	-29	5	0	0	-5	15	3	0	26	-21	37	22	16	-76	5	-83	-3	-8	-1	2	-40	14	22	-8	0	50
6		1,25	no	0,45	0,48	0	0	0	20	-3	-26	11	0	0	-17	2	-3	0	8	-26	0	31	16	-95	2	-79	-5	23	-1	3	-23	15	6	-5	0	21
7	Rear Leg Impact Cases	0,58	yes	0,60	0,45	11	0	0	6	-6	-15	18	0	0	2	0	-8	0	-9	-15	50	44	32	-98	-6	-83	-4	0	-17	-17	-27	-9	52	-10	0	21
8		2,28	no	0,47	0,45	0	0	0	-2	11	6	15	-1	0	-1	0	-4	-1	2	-48	-24	11	42	-56	-27	-120	1	-52	-12	6	-22	0	43	7	0	45
9		2,91	yes	0,46	0,49	0	19	0	3	8	-4	17	-2	0	1	0	-8	-2	9	-34	-30	39	17	-121	3	-68	-8	-9	-1	15	-34	7	86	-7	-26	30
10		2,04	no	0,45	0,40	9	0	0	15	-8	-7	21	2	0	1	0	-6	3	-35	-9	20	47	39	-92	-20	-76	9	8	6	0	-39	6	30	-15	0	34
11		-0,14	yes	0,46	0,42	6	0	0	33	-28	-35	17	0	0	0	0	-5	0	3	-13	36	17	-21	-31	-15	-34	-2	4	8	1	-34	-4	51	-16	0	25
12		1,64	no	0,51	0,31	23	21	34	-1	-7	8	36	0	1	2	0	-4	0	63	-75	29	8	-31	-145	-9	-152	6	8	-11	-11	-30	-6	39	-20	0	-3
13		2,09	no	0,45	0,40	17	0	0	4	5	-3	14	-2	1	6	-10	7	-3	56	-12	66	15	-32	-155	9	-45	-10	-21	0	2	-32	-4	84	-38	0	44
14		1,80	no	0,53	0,48	7	0	0	0	9	-2	0	3	0	1	6	-5	4	0	-21	8	37	23	-61	3	-119	-4	-10	3	-8	-30	9	65	-18	0	41
15		0,92	yes	0,45	0,44	0	0	0	9	10	-9	2	-3	0	0	0	-4	-4	0	-13	66	85	35	-101	1	-97	-6	-37	-4	-7	-58	-2	86	-24	0	28
16	Baseline	0,00	no	0,50	0,51	0	0	0	0	0	0	0	0	0	0	0	2	0	-11	-13	-11	13	72	-56	-72	-56	0	8	-22	0	-10	0	0	0	0	4
17		-1,04	no	0,55	0,50	6	0	0	-1	4	-20	-3	-2	0	0	0	0	-2	-12	-16	21	23	38	-32	-36	-30	-2	-21	-11	0	-31	10	105	-15	0	50
18		1,71	no	0,50	0,54	-5	0	0	-2	5	-10	3	-2	0	-1	0	-4	-3	24	-21	24	21	11	-49	-8	-45	-6	-38	4	0	-24	8	97	-20	0	48
19		1,41	yes	0,45	0,48	0	0	0	-1	1	2	8	2	0	-1	0	-9	2	-22	-25	-33	14	0	-137	-23	-125	10	-33	14	4	6	3	28	-38	0	47
20		-0,16	no	0,57	0,46	-23	0	0	-5	1	14	5	1	0	0	-11	6	1	17	-31	-2	24	-147	77	-36	-66	4	-13	18	1	-4	35	10	-9	0	47
21		2,54	yes	0,46	0,51	0	0	0	1	5	-3	17	2	0	-1	0	-11	2	0	-97	0	114	0	-81	22	-84	0	-46	-7	3	-15	1	28	-4	0	68
22		2,38	no	0,48	0,47	0	0	0	-1	12	0	3	1	0	0	0	-4	7	0	-17	0	17	0	-34	0	-34	1	-19	-5	8	-8	-4	42	-11	0	80
23		2,26	no	0,47	0,44	14	0	0	1	6	-4	-3	-1	0	0	0	-2	-1	46	-17	-19	11	9	-64	-36	-65	1	-27	-5	-1	-34	0	41	-16	0	83
24		1,38	no	0,51	0,46	0	0	0	3	-1	-5	6	-1	0	-1	0	-5	-1	12	-14	-13	15	0	-26	17	-21	-4	-26	1	2	8	4	35	-29	0	34
25		0,99	no	0,54	0,34	-9	0	0	0	5	0	3	-1	0	-1	0	1	-1	0	-14	16	18	-57	-31	4	-74	-3	-35	-1	-7	3	9	53	-22	0	36
26		1,37	yes	0,45	0,51	17	0	0	8	0	-9	-5	2	0	-1	-6	29	2	16	-14	8	17	20	-79	-26	-98	-10	-41	-6	-4	-11	-2	53	-25	0	24
27		0,50	yes	0,48	0,43	0	0	0	12	-3	-11	9	1	0	0	0	1	1	36	-11	16	12	-7	-68	-35	-76	1	-13	-12	-1	-11	17	24	-10	0	52
28	Forward Leg Impact Cases	1,00	yes	0,44	0,48	0	0	0	3	5	-4	8	0	0	0	0	1	0	-44	0	-32	0	23	-126	-28	-138	6	-24	2	1	-11	-3	63	-17	0	18
29		0,00	yes	0,50	0,55	0	0	0	-2	11	1	11	-1	1	1	0	4	-1	0	-12	0	12	27	-138	-15	-135	2	-10	12	0	-38	3	26	-18	0	83
30		0,00	no	0,50	0,44	0	0	0	12	5	-13	7	-1	0	-1	0	2	-2	-7	-24	0	12	13	-94	154	124	7	-31	-2	11	-26	10	39	2	0	50
31		1,54	no	0,53	0,55	0	0	0	24	-4	-31	6	-2	1	0	0	-3	-2	0	-13	0	15	0	-26	-9	-26	-3	-32	0	-2	-1	-3	33	-5	0	19
32		0,00	no	0,64	0,43	0	0	0	2	-5	0	12	-1	9	-2	0	4	-1	3	-38	-14	14	93	-35	-46	-50	-3	-38	-22	2	-4	1	34	1	0	53
33		2,64	no	0,50	0,48	0	0	0	14	-10	-15	-4	-18	-2	0	0	11	7	0	-13	19	17	25	-75	24	-43	2	-58	6	15	-47	9	81	0	-6	62
34		1,99	no	0,68	0,32	0	0	0	-1	4	-5	0	-1	0	0	0	-1	-1	7	-16	0	11	4	-10	-33	-41	-4	-32	-8	-2	5	-1	36	10	0	43
35		1,64	no	0,53	0,51	0	0	0	8	9	-8	8	0	0	-1	0	-6	-1	-20	-13	48	27	180	110	-21	-19	-8	-65	-5	-3	-16	3	103	-23	0	52
36		0,00	no	0,45	0,32	11	0	0	14	3	1	35	-1	0	-1	0	-6	-2	-12	-22	-38	3	3	-136	-61	-111	-6	-38	-14	-3	5	-9	31	-17	0	41
37		-0,43	no	0,57	0,40	69	0	0	1	4	5	37	4	18	1	0	0	4	-51	-20	16	17	26	-130	7	-151	-23	-8	-27	-8	-35	-15	33	-40	0	70
38		0,20	no	0,54	0,56	11	0	0	0	0	0	-17	2	0	-1	-9	21	2	-5	-7	35	25	26	-53	-13	-102	3	-49	9	9	18	1	103	-37	0	14
39		1,96	no	0,60	0,59	-23	0	0	4	-5	4	17	-4	0	0	0	4	-5	27	-33	-30	19	-3	-117	-13	-126	5	-41	0	-13	12	13	39	-22	0	19
40		3,02	no	0,50	0,52	0	0	0	2	-7	-10	-4	4	0	0	0	21	4	42	-66	51	60	-28	-44	-25	-18	23	-44	-12	14	-2	24	46	-35	0	103
41		1,70				17	0	0	-2	4	5	-1	0	0	1	0	7	0	-13	-9	-3	13	32	-117	125	132	3	-28	-10	3	-21	-7	52	-7	0	68